Materials Chemistry and Physics 276 (2022) 125337

Contents lists available at ScienceDirect

Materials Chemistry and Physics

journal homepage: www.elsevier.com/locate/matchemphys

TiO_2 nanotube layers decorated by titania nanoparticles as anodes for Li-ion microbatteries

Hanna Sopha [a,b,1], Clement Ghigo [c,d,1], Siowwoon Ng [b], Mahnaz Alijani [a,b], Ludek Hromadko [a,b], Jan Michalicka [b], Thierry Djenizian [c,e], Jan M. Macak [a,b,*]

[a] Center of Materials and Nanotechnologies, Faculty of Chemical Technology, University of Pardubice, Nam. Cs. Legii 565, 53002, Pardubice, Czech Republic
[b] Central European Institute of Technology, Brno University of Technology, Purkyňova 123, 612 00, Brno, Czech Republic
[c] Mines Saint-Etienne, Center of Microelectronics in Provence, Flexible Electronics Department, 13541, Gardanne, France
[d] Pellenc Energy S.A.S., Quartier Notre Dame, Route de Cavaillon, 84120 Pertuis, France
[e] Al-Farabi Kazakh National University, Center of Physical-Chemical Methods of Research and Analysis, Tole bi str., 96A, Almaty, Kazakhstan

HIGHLIGHTS

- TiO_2 nanotube layers were decorated with TiO_2 nanoparticles (NPs) by wet chemistry.
- The resulting structure was used for the first time as anode in Li-ion microbattery.
- A significant increase in areal capacity is shown for an optimized amount of NPs.
- The areal capacity was stable over 200 charge/discharge cycles.
- A Coulombic efficiency of 99.8% was obtained using optimized NP amount.

ARTICLE INFO

Keywords:
TiO_2 nanotube layers
TiO_2 nanoparticles
Decoration
Li-ion microbatteries

ABSTRACT

In this work, the utilization of TiO_2 nanotube (TNT) layers decorated with TiO_2 nanoparticles (NPs) as anodes in Li-ion microbatteries is reported for the first time. Such TiO_2 NPs decorated TNT layers possess an increased amount of active material and a higher surface area compared with their non-decorated (blank) counterparts. TNT layers decorated with several different amounts of TiO_2 NPs were tested by galvanostatic cycling tests. The capacities of the TiO_2 NPs decorated TNT layer anodes increase with the amount of NPs decoration due to the enhancement of the capacitive effect. Indeed, an areal capacity of ~126 μAh cm^{-2} (vs 88 μAh cm^{-2} for the non-decorated TNT layer) at the 200th cycle has been obtained after optimizing the NPs loading. On the other hand, a too high NPs loading of the TNT layers leads to a reduced areal capacity due to clogging of the nanotube exteriors and a significant decrease in inner diameter of the nanotubes.

1. Introduction

The raising demand of microelectromechanical systems (MEMs) in different fields, such as biological and medical applications or sensors, possesses a great challenge for scientists to develop power devices on the microscale with increased power and energy density as well as a long life-time [1–3]. Possible power devices for MEMs are, for instance, rechargeable Li-ion microbatteries (μLIBs). However, planar μLIBs do not fulfill the requirements of showing a high energy density [4]. Thus, in the recent years 3D μLIBs were introduced as an alternative to planar μLIBs to overcome this problem. For such 3D μLIBs, nanostructured electrodes, as for instance nanopillars, nanorods, or nanotubes, are widely explored due to their high areal capacity, large surface area, and short ion diffusion ways [5].

The most frequent anode material for (μ)LIBS is graphite. However, it suffers from safety concerns due to Li dendrite growth-induced short-circuits as the Li intercalation potential is rather low (~0.1 V vs Li/Li^{+}) [6]. A possible material to replace carbon is TiO_2, as it has a higher

* Corresponding author. Center of Materials and Nanotechnologies, Faculty of Chemical Technology, University of Pardubice, Nam. Cs. Legii 565, 53002, Pardubice, Czech Republic.

E-mail address: jan.macak@upce.cz (J.M. Macak).

[1] These authors contributed equally.

https://doi.org/10.1016/j.matchemphys.2021.125337
Received 6 August 2021; Received in revised form 29 September 2021; Accepted 6 October 2021
Available online 9 October 2021
0254-0584/

lithiation potential of ~1.6 V vs Li/Li^+ resulting in an enhanced safety. Furthermore, TiO_2 shows a good capacity retention upon cycling, low self-discharge, and low volume changes of less than 4% upon Li insertion/extraction from the lattice [2,7–9]. Many different TiO_2 nanostructures can be prepared, e.g. nanofibers [10], nanoparticles [11] or nanotubes [12]. Among these, anodic TiO_2 nanotube (TNT) layers gained great attention in the last two decades, as their fabrication is relatively easy, low-cost and their dimensions (e.g. diameter and TNT layer thickness) can be controlled by optimizing the electrolyte, as well as anodization potential and time [9,13,14]. Furthermore, these TNT layers have the advantage of being produced directly on a Ti substrate, which can be used as back contact for further applications without the need of additional immobilization of the TNTs on a conductive substrate. Due to the vertical alignment of the TNTs, anodic TNT layers possess additionally a direct diffusion pathway for the Li^+ ions resulting in a high performance [13,15]. Thus, in the recent years, pure and modified TNT layers have been extensively explored for their use as anodes in LIBs and all-solid-state μLIBs [7,16–29], as well as for other batteries systems [30–34].

The capacity of TNT layers can be further increased by coating or decorating them with secondary materials. These secondary materials can be of different composition and nature, as for instance coatings prepared by atomic layer deposition (ALD), such as ZnO, Al_2O_3 or MoS_2 [35–38], or a nanoparticle (NP) decoration, as Co_3O_4, NiO or Ag, using various different decoration methods [26,39–42]. While homogenous ALD coatings cover the whole TNT layer with the nanotubes' interiors being able to host possible volume expansions of the secondary material upon lithiation, a NP decoration does not just add a secondary material and increases mass and capacity, but additionally enhances the surface area of the TNT layers. Though TNT layers with NPs prepared from several different secondary materials have been employed as possible anodes for (μ)LIBs [26,39–42], somewhat surprisingly an additional decoration of TNT layers with TiO_2 NPs has not been shown yet in (μ) LIBS, although such decorations have been used already for dye-sensitized solar cells (DSSCs) or photocatalysis [43–46]. Such TiO_2 NP decoration can significantly increase the already high surface area and add additional mass to the electrode. Thus, the capacity of TNT layers decorated with NPs for μLIBS can be increased by the same material - TiO_2 - in the form of nanoparticles, without adding secondary materials, which could eventually possess some distinct disadvantages, such as high volume expansion upon lithiation or being toxic. A similar approach on TiO_2 NP decoration on hydrothermally prepared, non-ordered TNTs can be found in the literature [47]. However, as the TNTs were prepared hydrothermally and have completely disordered morphology; the Li-ion battery anode had to be prepared by mixing the TNTs with conductive carbon additives and a binder, and to be printed on a conducting support.

In this work, we employ for the first time TNT layers decorated with TiO_2 NPs of ~10 nm diameter as an anode in 3D μLIBs. It is shown that the areal capacity of the TiO_2 NP decorated TNT layers increases with an increase of the NPs loading of the TNT layers until an optimized amount of NPs was added. However, a too thick NP decoration clogs the exteriors of the nanotubes and as well decreases the diameter significantly. As a result, the surface area and thus the discharge capacity of the TNT layers decreases.

2. Material and methods

TNT layers (~5 μm thick with a diameter of ~230 nm) were prepared by anodizing Ti foils (Sigma-Aldrich, 127 μm thick) in an electrolyte consisting of 150 mM NH_4F and 10 vol% H_2O in ethylene glycol at 100 V for 4 h using a high-voltage potentiostat (PGU-200 V, Elektroniklabor GmbH) [48]. In the electrochemical cell, the Ti foil was used as anode and pressed against an o-ring leaving 1 cm^2 open to the electrolyte. A Pt foil was used as counter electrode. After anodization, the TNT layers were cleaned by sonication in isopropanol. The as-prepared amorphous TNT layers were further annealed at 400 °C for 1 h to receive anatase structure.

For the modification with TiO_2 NPs, the TNT layers were immersed into a 0.1 M $TiCl_4$ solution (ice-cooled), sonicated for 15 s, and stored at 70 °C for 30 min. Afterwards, the TNT layers were dried in air for ~20–30 min [46]. This sequence refers to 1 dip TiO_2 NPs and was repeated to receive 2, 3, 4, 7, and 10 dips TiO_2 NPs decorated TNT layers. After reaching the required TiO_2 NPs dips, the TNT layers were once more annealed at 400 °C for 30 min to transform the attached NPs into anatase TiO_2.

To study the electrochemical performance, the TNT layers were dried at 60 °C under vacuum for 12 h before entering an argon filled glovebox (MBraun LABStar) with <0.5 ppm H_2O and <0.5 ppm O_2 atmosphere. Batteries were assembled in two-electrode Swagelok cells with 150 μL of 1 M lithium hexafluorophosphate ($LiPF_6$) in ethylene carbonate (EC): dimethyl carbonate (DMC) 50/50 (%vol) organic liquid electrolyte. In the two-electrode set-up, a lithium foil served as a counter electrode, a Whatman glass microfiber paper with a thickness of 180 μm was used as a separator. Electrochemical tests were carried out at room temperature using a Biologic VMP3 potentiostat, equipped with EC-Lab software. Galvanostatic cycling tests with potential limitation (GCPL) were obtained at 1 C-rate in the potential window of 1–3 V vs. Li/Li^+. Cyclic voltammetry tests were performed in the same potential window at different scan rates of 0.25, 0.5, 0.75, 1.0 and 1.25 mV s^{-1}. The electrochemical impedance spectroscopy (EIS) experiments were conducted at open circuit potential (OCP). Measurements were carried out over frequencies ranging from 200 kHz to 10 mHz with a sine modulation of 10 mV. Following the electrochemical tests, each electrode underwent a two-step rinsing procedure in a Petri dish with pure DMC. The cleaning process was required to remove salt contamination for post-mortem morphological analysis.

The morphology of the TNT layers was characterized by a field-emission scanning electron microscope (FE-SEM, JEOL JSM 7500F, FEI Verios 460L) and an image corrected high-resolution transmission electron microscope (HR-TEM, FEI Titan Themis 60-300, operated at 300 keV) equipped with a high angle annular dark field detector for scanning transmission electron microscopy (HAADF-STEM) and Super-X energy dispersive X-ray (EDX) spectrometer. The structure was analyzed by X-ray diffraction (XRD, 45 kV, 40 mA) measurements (Panalytical Empyrean) using a Cu X-ray tube and a scintillation detector Pixcel3D.

3. Results and discussion

Fig. 1 shows SEM images of TNT layers with and without TiO_2 NP decoration. As one can see, the blank (non-decorated) TNT layers have a nanotube diameter of ~230 nm and a thickness of ~5 μm. The TNT layer decorated with 1 dip TiO_2 NPs reveals very few TiO_2 NPs. SEM images with higher magnifications can be found in Fig. S1. The amount of TiO_2 NPs increased with every additional dip into the $TiCl_4$ solution, with the open diameter of the nanotubes being reduced due to the occupancy of TiO_2 NPs. For the TNT layer decorated with 7 dips TiO_2 NPs, the exteriors between the nanotubes were completely clogged and the inner diameter was significantly decreased. However, the nanotube interiors were not clogged. An SEM image of a TNT layer decorated with 10 dips TiO_2 NPs is shown in Fig. S2. It can be seen that such high NP loading leads to a complete clogging of the TNT layer outside as well as inside individual nanotubes.

Cross-sectional SEM images of the TNT layers with TiO_2 NP decoration are shown in Fig. S3. Similar as on the top view images in Figs. 1 and S1, just very few nanoparticles can be seen for the TNT layer with 1 dip TiO_2 NPs. However, on TNT layers with TiO_2 NP decoration by higher numbers of dips, the NP decoration along the TNT walls and at the bottoms can clearly be seen. Thus, the complete TNT layers from the tops to the bottoms were decorated with TiO_2 NPs.

A homogenous distribution of the TiO_2 NPs was confirmed by TEM investigation of the 4 dips TiO_2 NP decorated TNT layer, as shown in

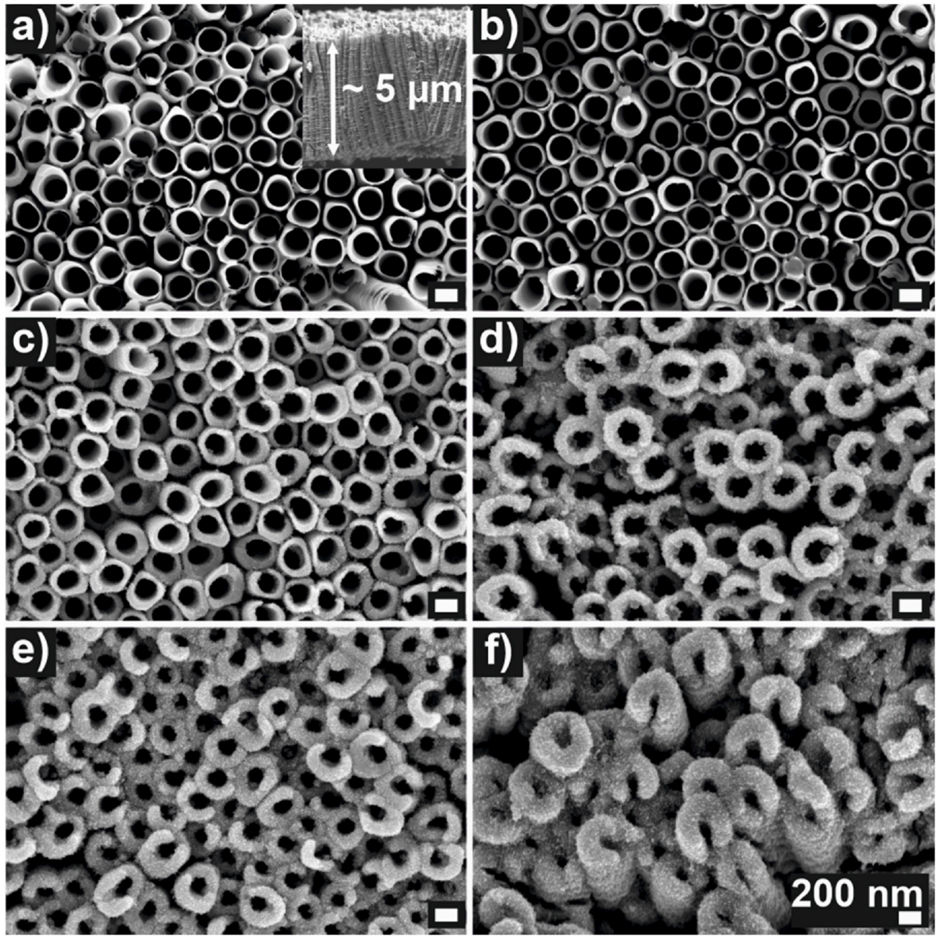

Fig. 1. SEM images of the a) blank TNT layer, and TNT layers decorated with b) 1 dip TiO_2 NPs, c) 2 dips TiO_2 NPs, d) 3 dips TiO_2 NPs, e) 4 dips TiO_2 NPs, and f) 7 dips TiO_2 NPs. The inset in part a) shows a cross section image of the TNT layer. All scale bars show 200 nm.

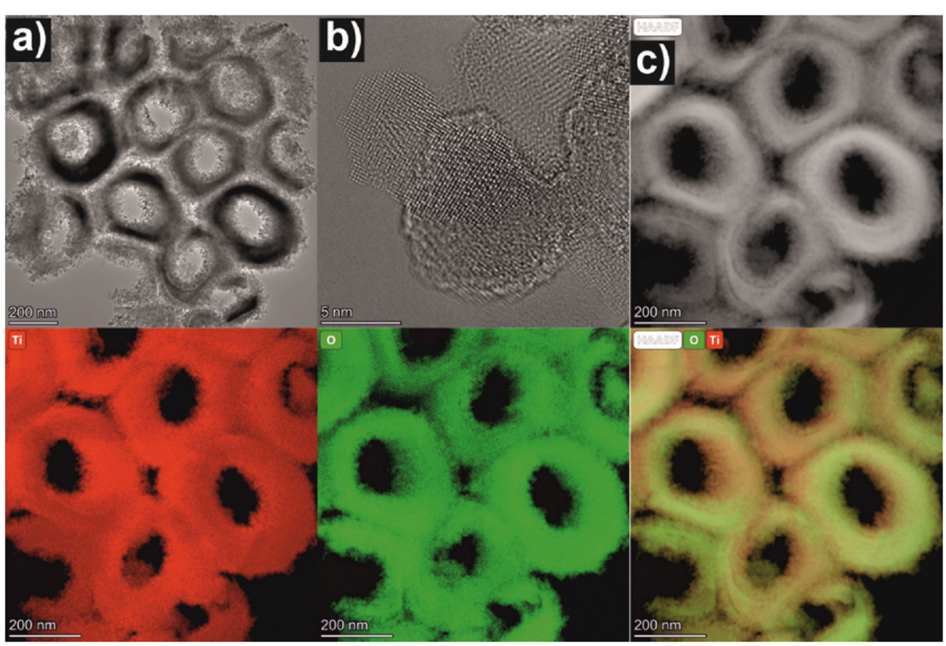

Fig. 2. a) TEM image of a fragment of a TNT layer decorated with 4 dips TiO_2 NPs, b) HR-TEM of a TiO_2 NP, c) HAADF-STEM image. The lower row shows the STEM EDX elemental maps with the distribution of Ti and O of the 4 dips TiO_2 NPs decorated TNT layer shown in part c).

Fig. 2. The NPs had a diameter of ~10 nm. As expected, XRD analysis (see Fig. S4) revealed that all TiO_2 NP decorated TNT layers are fully composed crystalline TiO_2 in anatase phase after the annealing procedure at 400 °C in air. The HR-TEM image in Fig. 2b shows one TiO_2 NP attached to the nanotube wall, confirming that the NPs are crystalline. The HAADF-STEM image in Fig. 2c shows a fragment of the nanotube layer, while a detailed EDX mapping of this fragment in the lower row of Fig. 2 reveals the equal distribution of Ti and O within the nanotubes.

Fig. 3a shows the effect of the increasing amount of TiO_2 NPs on the electrochemical performance of the TNT layer anodes for 3D μLIBs at a rate of 1 C for 20 cycles. It is apparent that the capacity values increased with the NP loading. The variations of the 1st discharge capacity ranging from 147 μAh cm^{-2} for the blank to 245 μAh cm^{-2} for the TNT layer decorated with 7 dips TiO_2 NPs can be at the first glance attributed to the increasing amount of the active material. Although the 1st irreversible capacity, i.e. the difference between the 2nd and 1st discharge capacity, can be observed for all TNT layers due to the formation of the solid electrolyte interphase (SEI) layer (as confirmed by the post-mortem analysis, see Fig. S5) and irreversible side reactions, the TNT layer decorated with 4 dips revealed unexpectedly the highest capacity value after 20 cycles. Indeed, the discharge capacity of the TNT layer decorated with 7 dips TiO_2 NPs dropped gradually during the cycling tests and only 53.6% of the initial capacity was retained while all other TNT layers showed good electrochemical behaviors with capacity retentions higher than 80% (i.e., the ratio between the capacity of the 20th charge/discharge cycle and the second discharge capacity). The exact values are given in Table 1. Thus, the control of the NP loading turned out to be crucial for the improvement of the electrochemical performance of the TNT layers. In order to investigate the electrochemical behaviors in more detail, charge/discharge experiments have been prolonged up to 200 cycles at the same kinetics for the blank and the TNT layers decorated with 4 dips and 7 dips TiO_2 NPs, as these TNT layers showed significant differences in areal capacity during the initial 20 cycles. The variation of the discharge capacity values *vs* cycling number, given in Fig. 3b, confirms the tendency observed for the initial 20 cycles. The TNT layer decorated with 4 dips TiO_2 NPs exhibited the highest capacity of 126 μAh cm^{-2} with a Coulombic Efficiency (CE) of 99.8%, while the TNT layer decorated with 7 dips TiO_2 NPs, reaching 72 μAh cm^{-2}, could retain only 37.6% of the initial capacity. Remarkably, the highest NP loading had a negative influence on the storage properties of the TNT layers as the capacity of the TNT layer decorated with 7 dips TiO_2 became lower than that of the blank TNT layer after 30 charge/discharge cycles. This might be attributed to the entire clogging of nanotube exteriors and a strong decrease of the nanotube diameter, resulting in a significant decrease of the accessible surface area. To confirm this expectation, the influence of the nanoparticle decoration on the specific area of nanotubes has been evidenced by electrochemical impedance spectroscopy (EIS) (Fig. 4). As the electrode resistance depends on its surface (R ~ 1/S), EIS spectra obtained before cycling experiments reveal that the resistance of the nanotube layers decreased after 4 dips but became higher than of the bare layer after 7 dips. Compared to the blank TNT layer, TNT layer decorated by 4 dips TiO_2

Table 1
Main electrochemical characteristics. Q – Capacity, CE – Coulombic efficiency, IC – 1st irreversible capacity, CR – Capacity retention.

		Blank	1 dip NPs	2 dips NPs	3 dips NPs	4 dips NPs	7 dips NPs
Cycle #1	*Q (μAh cm^{-2})*	147	155	173	181	225	245
	CE (%)	68.7	73.3	70.7	73.2	73.1	75.5
Cycle #2	*Q (μAh cm^{-2})*	109	117	132	141	170	191
	CE (%)	90.2	92.4	91.1	91.8	92.7	92.7
	IC (μAh cm^{-2})	38.0	37.9	40.9	40.6	55.3	54.3
Cycle#20	*Q (μAh cm^{-2})*	97	103	111	123	143	102
	CE (%)	98.4	99.3	98.5	98.6	98.9	98.5
	CR (%)	88.5	88.1	83.9	87.6	84.1	53.6
Cycle #100	*Q (μAh cm^{-2})*	84	–	–	–	122	71
	CE (%)	99.7	–	–	–	99.8	99.9
	CR (%)	86.0	–	–	–	72.1	37.3
Cycle #150	*Q (μAh cm^{-2})*	92	–	–	–	126	71
	CE (%)	99.8	–	–	–	99.8	99.6
	CR (%)	84.6	–	–	–	74.0	37.2
Cycle #200	*Q (μAh cm^{-2})*	88	–	–	–	126	72
	CE (%)	99.8	–	–	–	99.8	99.6
	CR (%)	81	–	–	–	74.1	37.6

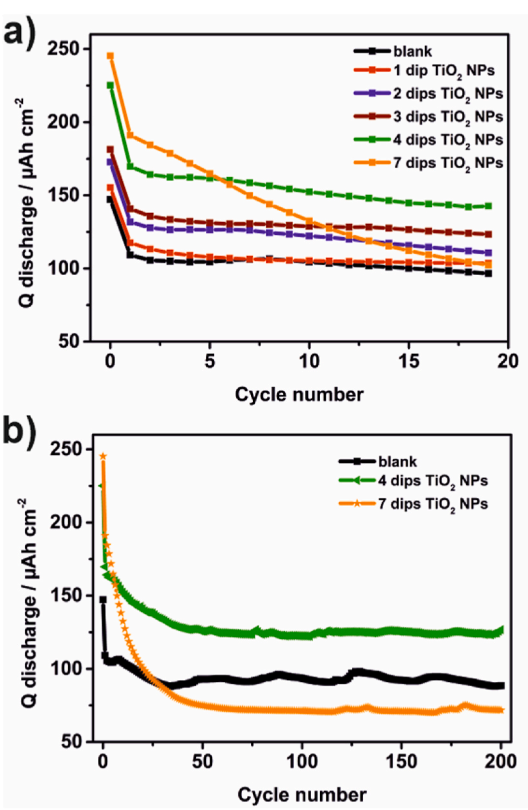

Fig. 3. Discharge capacity values of blank and TiO_2 NPs decorated TNT layers at 1C for a) 20 cycles and b) 200 cycles.

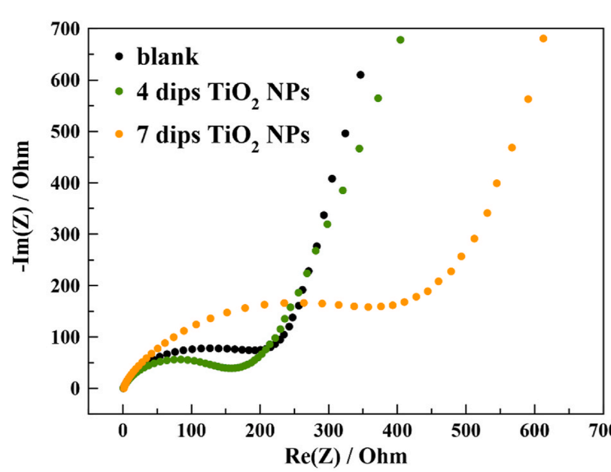

Fig. 4. EIS spectra of the blank, 4 dips and 7 dips TiO_2 NPs decorated TNT layers before cycling experiments.

NPs offers a bigger surface area while the TNT layer decorated by 7 dips TiO_2 NPs leads a lower one. The main electrochemical results obtained from the cycling tests are summarized in Table 1.

It must be noted that the areal capacity of the blank TNT layer appears lower compared to our previous studies [37,38]. This is, however, attributed to different nanotube dimension used in this study (diameter ~230 nm, thickness ~5 μm) while in our previous studies TNT layers with a diameter of ~130 nm and a thickness ~20 μm were employed. Thus, the specific area of the TNT layers used in this study was significantly smaller. When comparing the areal capacity of non-modified samples herein and in the previous studies per 1 μm of the TNT layer thickness after 100 charge/discharge cycles, similar values were received, i.e. ~17 μAh cm^{-2} $μm^{-1}$ for the 5 μm thick TNT layers in this study and ~11 μAh cm^{-2} $μm^{-1}$ for the 20 μm thick TNT layers in the previous studies [37,38]. The differences per 1 μm can be attributed to different thicknesses of the TNT walls.

The observed electrochemical characteristics and trends can be explained by a competition between the increase of active material mass and the modification of the specific area of the TNT layers. Owing to the spherical morphology of the added NPs, the walls of the TNT layers decorated with TiO_2 NPs offered a larger surface area, compared to the blank TNT layers, that can enhance the storage of charge in the outer part of both tubes and NPs as long as the porosity of nanotubes is preserved. Thus, the capacitive effect involving the non-faradaic reaction of Li^+ at the surface of TiO_2 was less predominant for the TNT layer decorated with 7 dips TiO_2 NPs, as the nanotubes were almost clogged by the huge amount of NPs. In addition, the SEI formation occurring during the first cycling tests probably plugged the nanotubes completely, leading to poor electrochemical performance after 50 cycles. It can also be noticed that the 1st irreversible capacity is higher for decorated nanotubes, which is consistent with the increase of the nanotube surface leading to the increase of reaction sites promoting the SEI formation.

In order to explain the higher performance of the TNT layer decorated with 4 dips TiO_2 NPs compared to the other TNT layers and to obtain insights into the electrochemical behavior, cyclic voltammetry (CV) was performed. Fig. 5a and b displays the CV curves of the blank TNT layer and the TNT layer decorated with 4 dips TiO_2 NPs. During the reduction process, the peaks centered at 1.6 V can be attributed to the Li^+ insertion into anatase TiO_2, while the anodic peaks around 2.2 V are ascribed to the Li^+ extraction [16,36,49]. As the sweep rate increases, there is a noticeable peak shift from higher to lower potentials for Li^+ insertion and inversely for the Li^+ extraction. The increase of the potential difference between the anodic and cathodic peaks is due to kinetic and ohmic drop effects. Compared to the blank TNT layer, higher current densities are registered for the TNT layer decorated with 4 dips TiO_2 NPs that can be explained by the added TiO_2 NPs attached to the TNT layers resulting in higher mass and higher surface area enhancing the capacitive effect. Thus, an enhanced Li^+ storage was obtained for the TNT layer decorated with 4 dips TiO_2 NPs.

Fig. 5c shows the variation of the anodic peak current, I_p, as a function of the scan rate, v, which can be used to determine, whether the storage mode occurs preferentially in the bulk ($I_p \propto v^{1/2}$) or at the surface ($I_p \propto v^1$). In the case of mixed Li^+ storage mechanism ($I_p \propto v^a$), the two contributions can be estimated by comparing the exponential values, a. The best fits of the I_p vs v using an apparent power-law dependence give exponential values of 0.51 for the blank and 0.58 for the TNT layer decorated with 4 dips TiO_2 NPs. The larger exponential value, deviating from 0.5 toward 1 for TNT layer decorated with 4 dips TiO_2 NPs confirms that the superior electrochemical performance is due to the enhancement of the capacitive effect as it has been already reported for TNTs and other systems [50,51].

Thus, it can be summarized that the TiO_2 NPs decoration of the TNT layers can promote the areal capacity as long as the nanotubular morphology is preserved.

Post-cycling SEM analysis is shown in Fig. S5 for the TNT layer decorated with 1 dip TiO_2 NPs. As one can see, a SEI layer was formed on the TNT layer as discussed above. However, after rinsing of the TNT layers with DMC the preserved nanotubular structure as well as the NPs decoration was observed for all TNT layers (Fig. S6). Thus, the SEI layers formed on the TNT layers were washed out during the short washing step in DMC after the cycling test to remove the rests of the electrolyte. Fig. S7 shows post-cycling XRD analysis of the TNT layers with and without NP decoration. In all cases, pure TiO_2 phases were detected, i.e. without any $Li_xTi_yO_z$.

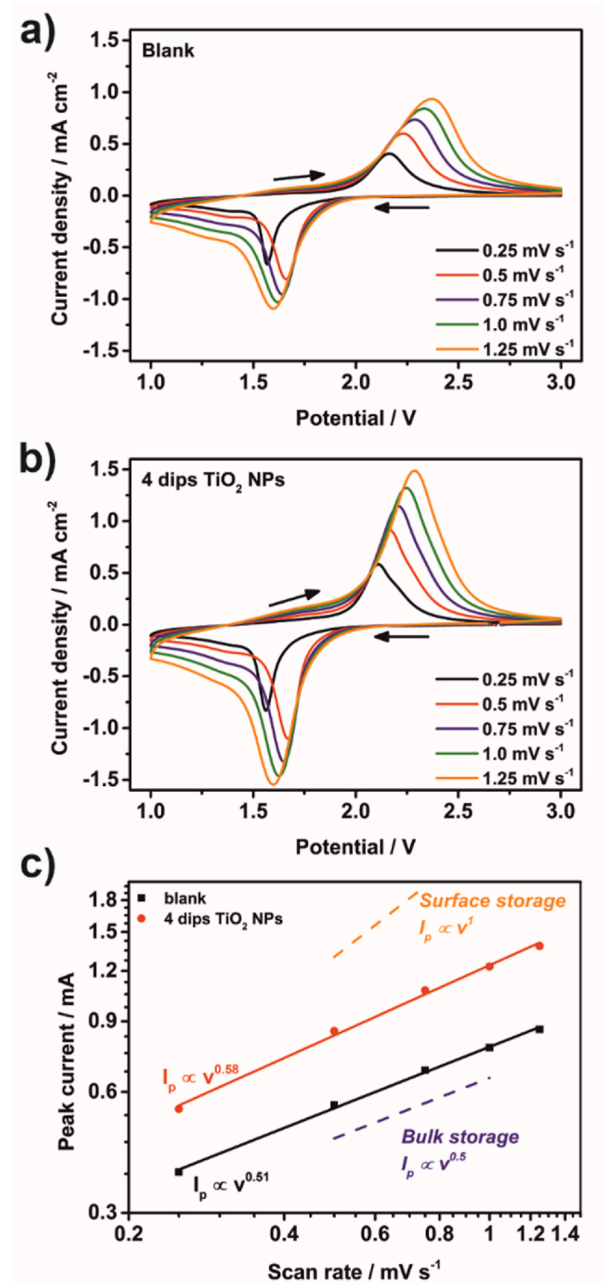

Fig. 5. CV curves of the a) blank TNT layer and b) TNT layer decorated with 4 dips TiO_2 NPs recorded at various scan rates, and c) variation of the anodic peak current vs. scan rate for the blank and TNT layer decorated with 4 dips TiO_2 NPs.

Fig. 6a shows post-cycling TEM investigations of TNT layer decorated with the 4 dips TiO_2 NPs. A homogenous distribution of the ~10 nm large TiO_2 NPs between the nanotubes can be seen even after 200 charge/discharge cycles. This confirms the stability of TiO_2 NPs on the

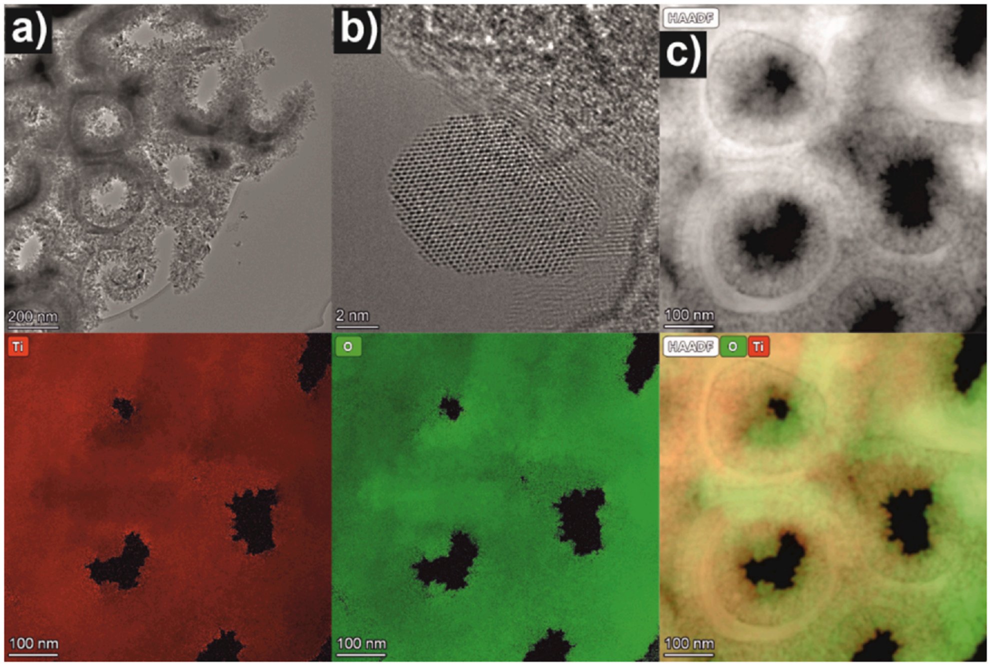

Fig. 6. a) Post-mortem TEM image of a fragment of a TNT layer decorated with 4 dips TiO_2 NPs, b) post-mortem HR-TEM of a TiO_2 NP, c) post-mortem HAADF-STEM image. The lower row shows the STEM EDX elemental maps with the distribution of Ti and O of the 4 dips TiO_2 NPs decorated TNT layer shown in part c).

TNT layer. Fig. 6b shows a HR-TEM image of one TiO_2 NP attached to the nanotube wall, showing that the NP is crystalline. Fig. 6c shows the HAADF-STEM image of a fragment of the nanotube layer. A detailed EDX mapping of this fragment in the lower row of the figure reveals the equal distribution of Ti and O within the nanotubes. Other elements were not detected. Overall, the comparison of TEM/STEM and EDX results between Figs. 2 and 6 clearly confirms, that TNT layers with decorated TiO_2 NPs did not undergo any change upon cycling.

4. Conclusions

In summary, a beneficial effect of the use of TiO_2 NPs decorated TNT layers as anode in 3D μLIBs was shown for the first time. Compared to blank TNT layers, the TiO_2 NPs decorated TNT layers with a moderate loading of NPs showed an increased areal capacity over 200 charge/discharge cycles, due to an increase of active material and surface area. However, if the NP loading was too high a strong decline in areal capacity was observed during the first ~30 charge/discharge cycles. The approach shown here can be very important for the further fabrication of 3D μLIBs for small devices as it significantly enhances the performance of the TNT layers used as anodes.

CRediT authorship contribution statement

Hanna Sopha: TNT layer production, data evaluation, writing of the manuscript. **Clement Ghigo:** battery test, data evaluation, writing of the manuscript. **Siowwoon Ng:** NP decoration of the TNT layers, SEM investigations. **Mahnaz Alijani:** NP decoration of the TNT layers, SEM investigations. **Ludek Hromadko:** SEM investigation, XRD analysis. **Jan Michalicka:** TEM investigation. **Thierry Djenizian:** data evaluation, editing, Funding acquisition, Supervision. **Jan M. Macak:** data evaluation, editing, Funding acquisition, Supervision. The manuscript was written through contributions of all authors. All authors have read and revised the manuscript and given approval to the final version.

Declaration of competing interest

The authors declare that they have no known competing financial interests or personal relationships that could have appeared to influence the work reported in this paper.

Acknowledgements

The authors acknowledge the Ministry of Education, Youth and Sports of the Czech Republic (MEYS CR, LM 2018103, CZ.02.1.01/0.0/0.0/17_048/0 0 07421). The CzechNanoLab project LM2018110 funded by MEYS CR is gratefully acknowledged for the financial support of TEM and SEM investigations at CEITEC Nano Research Infrastructure.

Pellenc Energy and Mines Saint-Etienne are acknowledged for financial supports.

Appendix A. Supplementary data

Supplementary data to this article can be found online at https://doi.org/10.1016/j.matchemphys.2021.125337.

References

[1] P.H.L. Notten, F. Roozeboom, R.A.H. Niessen, L. Baggetto, 3-D integrated all-solid-state rechargeable batteries, Adv. Mater. 19 (2007) 4564–4567, https://doi.org/10.1002/adma.200702398.
[2] T. Djenizian, I. Hanzu, P. Knauth, Nanostructured negative electrodes based on titania for Li-ion microbatteries, J. Mater. Chem. 21 (2011) 9925–9937, https://doi.org/10.1039/c0jm04205f.
[3] J.H. Pikul, H. Gang Zhang, J. Cho, P.V. Braun, W.P. King, High-power lithium ion microbatteries from interdigitated three-dimensional bicontinuous nanoporous electrodes, Nat. Commun. 4 (2013) 1732, https://doi.org/10.1038/ncomms2747.
[4] C. Yue, J. Li, L. Lin, Fabrication of Si-based three-dimensional microbatteries: a review, Front. Mech. Eng. Times 12 (2017) 459–476, https://doi.org/10.1007/s11465-017-0462-x.
[5] B.L. Ellis, P. Knauth, T. Djenizian, Three-Dimensional self-supported metal oxides for advanced energy storage, Adv. Mater. 26 (2014) 3368–3397, https://doi.org/10.1002/adma.201306126.
[6] A.R. Armstrong, G. Armstrong, J. Canales, P.G. Bruce, TiO2–B nanowires as negative electrodes for rechargeable lithium batteries, J. Power Sources 146 (2005) 501–506, https://doi.org/10.1016/j.jpowsour.2005.03.057.
[7] G.F. Ortiz, I. Hanzu, T. Djenizian, P. Lavela, J.L. Tirado, P. Knauth, Alternative Li-ion battery electrode based on self-organized titania nanotubes, Chem. Mater. 21 (2009) 63–67, https://doi.org/10.1021/cm801670u.
[8] J.R. González, R. Alcántara, F. Nacimiento, G.F. Ortiz, J.L. Tirado, E. Zhecheva, R. Stoyanova, Long-length titania nanotubes obtained by high-voltage anodization

and high-intensity ultrasonication for superior capacity electrode, J. Phys. Chem. C 116 (2012) 20182–20190, https://doi.org/10.1021/jp3050115.

[9] K. Lee, A. Mazare, P. Schmuki, One-dimensional titanium dioxide nanomaterials: Nanotubes, Chem. Rev. 114 (2014) 9385–9454, https://doi.org/10.1021/cr500061m.

[10] S. Yoo, S.A. Akbar, K.H. Sandhage, Nanocarving of bulk titania crystals into oriented arrays of single-crystal nanofibers via reaction with hydrogen-bearing gas, Adv. Mater. 16 (2004) 260–264, https://doi.org/10.1002/adma.200305781.

[11] E. Scolan, C. Sanchez, Synthesis and characterization of surface-protected nanocrystalline titania particles, Chem. Mater. 10 (1998) 3217–3223, https://doi.org/10.1021/cm980322q.

[12] V. Zwilling, M. Aucouturier, E. Darque-Ceretti, Anodic oxidation of titanium and TA6V alloy in chromic media. An electrochemical approach, Electrochim. Acta 45 (1999) 921–929, https://doi.org/10.1016/S0013-4686(99)00283-2.

[13] J.M. Macak, H. Tsuchiya, A. Ghicov, K. Yasuda, R. Hahn, S. Bauer, P. Schmuki, TiO2 nanotubes: self-organized electrochemical formation, properties and applications, Curr. Opin. Solid State Mater. Sci. 11 (2007) 3–18, https://doi.org/10.1016/j.cossms.2007.08.004.

[14] M.-M. Zhang, J.-Y. Chen, H. Li, C.-R. Wang, Recent progress in Li-ion batteries with TiO2 nanotube anodes grown by electrochemical anodization, Rare Met. 40 (2021) 249–271, https://doi.org/10.1007/s12598-020-01499-x.

[15] H. Han, T. Song, E.-K. Lee, A. Devadoss, Y. Jeon, J. Ha, Y.-C. Chung, Y.-M. Choi, Y.-G. Jung, U. Paik, Dominant factors governing the rate capability of a TiO 2 nanotube Anode for high power lithium ion batteries, ACS Nano 6 (2012) 8308–8315, https://doi.org/10.1021/nn303002u.

[16] G.F. Ortiz, I. Hanzu, P. Knauth, P. Lavela, J.L. Tirado, T. Djenizian, TiO2 nanotubes manufactured by anodization of Ti thin films for on-chip Li-ion 2D microbatteries, Electrochim. Acta 54 (2009) 4262–4268, https://doi.org/10.1016/j.electacta.2009.02.085.

[17] G.D. Salian, C. Lebouin, A. Demoulin, M.S. Lepihin, S. Maria, A.K. Galeyeva, A. P. Kurbatov, T. Djenizian, Electrodeposition of polymer electrolyte in nanostructured electrodes for enhanced electrochemical performance of thin-film Li-ion microbatteries, J. Power Sources 340 (2017) 242–246, https://doi.org/10.1016/j.jpowsour.2016.11.078.

[18] M. Braglia, I.V. Ferrari, T. Djenizian, S. Kaciulis, P. Soltani, M.L. Di Vona, P. Knauth, Bottom-up electrochemical deposition of poly(styrene sulfonate) on nanoarchitectured electrodes, ACS Appl. Mater. Interfaces 9 (2017) 22902–22910, https://doi.org/10.1021/acsami.7b04335.

[19] M.C. López, G.F. Ortiz, J.R. González, R. Alcántara, J.L. Tirado, Improving the performance of titania nanotube battery materials by surface modification with lithium phosphate, ACS Appl. Mater. Interfaces 6 (2014) 5669–5678, https://doi.org/10.1021/am500189h.

[20] R. Menéndez, P. Alvarez, C. Botas, F. Nacimiento, R. Alcántara, J.L. Tirado, G. F. Ortiz, Self-organized amorphous titania nanotubes with deposited graphene film like a new heterostructured electrode for lithium ion batteries, J. Power Sources 248 (2014) 886–893, https://doi.org/10.1016/j.jpowsour.2013.10.019.

[21] M. Zhang, C. Wang, H. Li, J. Wang, M. Li, X. Chen, Enhanced performance of lithium ion batteries from self-doped TiO2 nanotube anodes via an adjustable electrochemical process, Electrochim. Acta 326 (2019) 134972, https://doi.org/10.1016/j.electacta.2019.134972.

[22] W. Wei, G. Oltean, C.-W. Tai, K. Edström, F. Björefors, L. Nyholm, High energy and power density TiO2 nanotube electrodes for 3D Li-ion microbatteries, J. Mater. Chem. 1 (2013) 8160, https://doi.org/10.1039/c3ta11273j.

[23] J. Brumbarov, J. Kunze-Liebhäuser, Silicon on conductive self-organized TiO2 nanotubes – a high capacity anode material for Li-ion batteries, J. Power Sources 258 (2014) 129–133, https://doi.org/10.1016/j.jpowsour.2014.02.049.

[24] M. Madian, L. Giebeler, M. Klose, T. Jaumann, M. Uhlemann, A. Gebert, S. Oswald, N. Ismail, A. Eychmüller, J. Eckert, Self-Organized TiO 2/CoO nanotubes as potential anode materials for lithium ion batteries, ACS Sustain. Chem. Eng. 3 (2015) 909–919, https://doi.org/10.1021/acssuschemeng.5b00026.

[25] S.-H. Kim, S.-Y. Choi, Fabrication of Cu-coated TiO2 nanotubes and enhanced electrochemical performance of lithium ion batteries, J. Electroanal. Chem. 744 (2015) 45–52, https://doi.org/10.1016/j.jelechem.2015.03.007.

[26] G. Du, Z. Guo, P. Zhang, Y. Li, M. Chen, D. Wexler, H. Liu, SnO2nanocrystals on self-organized TiO2 nanotube array as three-dimensional electrode for lithium ion microbatteries, J. Mater. Chem. 20 (2010) 5689–5694, https://doi.org/10.1039/c0jm00330a.

[27] H. Fraoucene, V.A. Sugiawati, D. Hatem, M.S. Belkaid, F. Vacandio, M. Eyraud, M. Pasquinelli, T. Djenizian, Optical, Electrochemical Properties, Of self-organized TiO2 nanotube Arrays from anodized Ti−6Al−4V alloy, Front. Chem. 7 (2019) 1–9, https://doi.org/10.3389/fchem.2019.00066.

[28] N. Plylahan, M. Letiche, M.K. Samy Barr, B. Ellis, S. Maria, T.N.T. Phan, E. Bloch, P. Knauth, T. Djenizian, High energy and power density TiO2 nanotube electrodes for single and complete lithium-ion batteries, J. Power Sources 273 (2015) 1182–1188, https://doi.org/10.1016/j.jpowsour.2014.09.152.

[29] G.D. Salian, B.M. Koo, C. Lefevre, T. Cottineau, C. Lebouin, A.T. Tesfaye, P. Knauth, V. Keller, T. Djenizian, Niobium alloying of self-organized TiO2 nanotubes as an anode for lithium-ion microbatteries, Adv. Mater. Technol. 3 (2018) 1700274. https://onlinelibrary.wiley.com/doi/pdf/10.1002/admt.201700274.

[30] M. Cabello, G.F. Ortiz, M.C. López, R. Alcántara, J.R. González, J.L. Tirado, R. Stoyanova, E. Zhecheva, Self-organized sodium titanate/titania nanoforest for the negative electrode of sodium-ion microbatteries, J. Alloys Compd. 646 (2015) 816–826, https://doi.org/10.1016/j.jallcom.2015.06.183.

[31] J.R. Gonzales, R. Alcantara, F. Nacimiento, G.F. Ortiz, J.L. Tirado, Improving the electrochemistry of anatase for sodium ion batteries by using self- organized TiO2 nanotubes prepared by anodization under variable voltage, ECS Trans. 62 (2014) 45–56, https://doi.org/10.1039/B601073C.

[32] J.R. González, R. Alcántara, F. Nacimiento, G.F. Ortiz, J.L. Tirado, Self-Organized, anatase, double-walled nanotubes prepared by anodization under voltage ramp as negative electrode for aqueous sodium-ion batteries, J. Electrochem. Soc. 162 (2015) A3007–A3012, https://doi.org/10.1149/2.0021502jes.

[33] A. Auer, J. Kunze-Liebhäuser, Recent progress in understanding ion storage in self-organized anodic TiO 2 nanotubes, Small Methods 3 (2019) 1800385, https://doi.org/10.1002/smtd.201800385.

[34] G. Cha, S. Mohajernia, N.T. Nguyen, A. Mazare, N. Denisov, I. Hwang, P. Schmuki, Li + pre-insertion leads to formation of solid electrolyte interface on TiO2 nanotubes that enables high-performance anodes for sodium ion batteries, Adv. Energy Mater. 10 (2020) 1903448, https://doi.org/10.1002/aenm.201903448.

[35] R. Li, Z. Xie, H. Lu, D.W. Zhang, A. Yu, Fabrication of core-shell nanotube arrays as three-dimensional anode material for lithium ion batteries, Int. J. Electrochem. Sci. 8 (2013) 11118–11124. ZnO@TiO2.

[36] H. Sopha, G.D. Salian, R. Zazpe, J. Prikryl, L. Hromadko, T. Djenizian, J.M. Macak, ALD Al2O3 -coated TiO2 nanotube layers as anodes for lithium-ion batteries, ACS Omega 2 (2017) 2749–2756, https://doi.org/10.1021/acsomega.7b00463.

[37] A.T. Tesfaye, H. Sopha, A. Ayobi, R. Zazpe, J. Rodriguez-Pereira, J. Michalicka, L. Hromadko, S. Ng, Z. Spotz, J. Prikryl, J.M. Macak, T. Djenizian, TiO2 nanotube layers decorated with Al2O3/MoS2/Al2O3 as anode for li-ion microbatteries with enhanced cycling stability, Nanomaterials 10 (2020) 953, https://doi.org/10.3390/nano10050953.

[38] H. Sopha, A.T. Tesfaye, R. Zazpe, J. Michalicka, F. Dvorak, L. Hromadko, M. Krbal, J. Prikryl, T. Djenizian, J.M. Macak, ALD growth of MoS2 nanosheets on TiO2 nanotube supports, FlatChem 17 (2019) 100130, https://doi.org/10.1016/j.flatc.2019.100130.

[39] N.A. Kyerematenq, C. Lebouin, P. Knauth, T. Djenizian, The electrochemical behaviour of TiO2 nanotubes with Co3O4 or NiO submicron particles: composite anode materials for Li-ion micro batteries, Electrochim. Acta. 88 (2013) 814–820, https://doi.org/10.1016/j.electacta.2012.09.120.

[40] S.A. Pervez, U. Farooq, A. Yaqub, C.-H. Doh, D. Kim, S. Sim, M. Hwang, J.-H. Choi, Y.-J. Lee, Improved performance of Ag-nanoparticle-decorated TiO2 nanotube arrays in Li-ion batteries, J. Kor. Phys. Soc. 63 (2013) 1809–1814, https://doi.org/10.3938/jkps.63.1809.

[41] D. Guan, Y. Wang, Electrodeposition of Ag nanoparticles onto bamboo-type TiO2 nanotube arrays to improve their lithium-ion intercalation performance, Ionics 19 (2013) 879–885, https://doi.org/10.1007/s11581-012-0814-9.

[42] Y. Fan, N. Zhang, L. Zhang, H. Shao, J. Wang, J. Zhang, C. Cao, Co3O4-coated TiO2 nanotube composites synthesized through photo-deposition strategy with enhanced performance for lithium-ion batteries, Electrochim. Acta. 94 (2013) 285–293, https://doi.org/10.1016/j.electacta.2013.01.114.

[43] H. Chang, W. Tzeng, S. Cheng, Modification of TiO2 nanotube arrays by solution coating, Solid State Ionics 180 (2009) 817–821, https://doi.org/10.1016/j.ssi.2009.02.005.

[44] H. Mirabolghasemi, N. Liu, K. Lee, P. Schmuki, Formation of 'single walled' TiO2 nanotubes with significantly enhanced electronic properties for higher efficiency dye-sensitized solar cells, Chem. Commun. 49 (2013) 2067–2069, https://doi.org/10.1039/c3cc38793c.

[45] S. So, I. Hwang, P. Schmuki, Hierarchical DSSC structures based on "single walled" TiO2 nanotube arrays reach a back-side illumination solar light conversion efficiency of 8%, Energy Environ. Sci. 8 (2015) 849–854, https://doi.org/10.1039/C4EE03729D.

[46] H. Sopha, M. Krbal, S. Ng, J. Prikryl, R. Zazpe, F.K. Yam, J.M. Macak, Highly efficient photoelectrochemical and photocatalytic anodic TiO2 nanotube layers with additional TiO2 coating, Appl. Mater. Today 9 (2017) 104–110, https://doi.org/10.1016/j.apmt.2017.06.002.

[47] X. Liu, Q. Sun, A.M.C. Ng, A.B. Djurišić, M. Xie, C. Liao, K. Shih, M. Vranješ, J. M. Nedeljković, Z. Deng, In situ synthesis of TiO 2 (B) nanotube/nanoparticle composite anode materials for lithium ion batteries, Nanotechnology 26 (2015) 425403, https://doi.org/10.1088/0957-4484/26/42/425403.

[48] S. Das, H. Sopha, M. Krbal, R. Zazpe, V. Podzemna, J. Prikryl, J.M. Macak, Electrochemical infilling of CuInSe2 within TiO2 nanotube layers and subsequent photoelectrochemical studies, ChemElectroChem. 4 (2017) 495–499, https://doi.org/10.1002/celc.201600763.

[49] G.D. Salian, M. Krbal, H. Sopha, C. Lebouin, M.-V. Coulet, J. Michalicka, L. Hromadko, A.T. Tesfaye, J.M. Macak, T. Djenizian, Self-supported sulphurized TiO_2 nanotube layers as positive electrodes for lithium microbatteries, Appl. Mater. Today 16 (2019), https://doi.org/10.1016/j.apmt.2019.05.015.

[50] N. Plylahan, A. Demoulin, C.L. Chrystelle Lebouin, P. Knauth, T. Djenizian, Mechanism study of Li+ insertion into titania nanotubes, RSC Adv. 5 (2015) 28474–28477, https://doi.org/10.1039/C5RA03759J.

[51] S. Ouendi, C. Arico, F. Blanchard, J.-L. Codron, X. Wallart, P.L. Taberna, P. Roussel, L. Clavier, P. Simon, C. Lethien, Synthesis of T-Nb2O5 thin-films deposited by Atomic Layer Deposition for miniaturized electrochemical energy storage devices, Energy Storage Mater. 16 (2019) 581–588, https://doi.org/10.1016/j.ensm.2018.08.022.